Journal of the Geological Survey of Brazil vol 1, no 1, 1-9, April 2018

Journal of the Geological Survey of Brazil

Gamma-ray attenuation caused by rainforest dispersion compared to Vegetation Index: estimates on the effects in airborne gamma-spectrometry data – example from the State of Rondônia, Amazonia, Brazil

Guilherme Ferreira da Silva[1]*, Michelle Cunha Graça[1]

[1] Serviço Geológico do Brasil – CPRM/SGB; Residência de Porto Velho. Avenida Lauro Sodré, 2561, São Sebastião, Porto Velho, RO. CEP: 76.801-581

Abstract

This work estimates and discusses the effects of the rainforest on the airborne gamma-spectrometric surveys, taking as case study an area in the center of the Rondônia State, Amazonia, northern Brazil, where wooded and deforested areas are frequently juxtaposed. The control of the wooded areas is made using Landsat satellite images, by the calculation of the Normalized Difference Vegetation Index (NDVI), which allows distinguishing between areas with low and high concentration of green leaves. The results show that, compared to the NDVI values for non-vegetated areas, there is an attenuation of the mean signal of this index in the rainforest areas corresponding up to 36% of the Total Count of Radiation (TC), 12% of potassium (K), 37% of equivalent thorium (eTh), and 29% of the equivalent uranium (eU) concentrations. In our interpretation, part of this effect might be caused by the radiation shielding of the biomass in rainforest areas. However, as a secondary effect for the gamma-spectrometry data processing, the canopy trees are considered on the Digital Elevation Model being used as a surface to calculate the distance between the source of radiation and the sensor, which causes a bias in the processing, underestimating the real flight height to the ground surface. This last effect could have been avoided if there were a Digital Terrain Model available for the area, which should be considered for the data processing. Improving the understanding about this phenomenon, an increase in the quality of the signal-to-noise ratio of airborne gamma-spectrometric data used for the quantitative land modeling may be achieved for regions where the presence of rainforests is significant such as the Amazon region northern Brazil.

Article Information

Publication type: Regular article
Submitted:22 February 2018
Accepted: 2 April 2018
Online pub. 20 April 2018
Editor(s): E.L. Klein, D.L. Castro

Keywords:
Gamma-ray spectrometry,
Radiometric attenuation,
Airborne survey,
Rainforest shielding

*Corresponding author
Guilherme Ferreira da Silva
E-mail address:
guilherme.ferreira@cprm.gov.br

1. Introduction

Potassium, uranium, and thorium are the only naturally occurring chemical elements whose radioactive decay produces gamma radiation with sufficient energy and intensity to be measured in airborne geophysical surveys (Minty et al. 1997). This property, associated to the fact that the radiogenic isotopes of these three elements are equally distributed among the stable isotopes in nature, makes the airborne gamma-spectrometry a reliable tool for modern geological mapping and for qualitative comparisons of the concentration and distribution of these elements in the land surface.

Airborne gamma-spectrometry survey has also become a useful tool for mineral exploration, geological and environmental surveys and for many other fields of the Earth Sciences.

In recent successful examples, geophysical data have been used to identify targets for mineral exploration, such as hydrothermal alteration halos, uranium occurrences, alkaline complexes or intrusions, such as kimberlites and carbonatites, and the presence of Th-Nb-REE-bearing minerals (Shives 2015; Elkhadragy et al. 2016; Saad 2017; Bedini and Rasmussen 2018). In addition, the use of radiometric airborne data for large scale geological and soil mapping has been improved with new techniques of non-supervised and quantitative processes in data integration (Perrotta et al. 2008; Beamish 2015; Iza et al. 2016) . However, the processing of airborne spectrometry data is not trivial and depends on many environmental factors that must be corrected for a standard interpretation, such as flight height, air and soil moisture, and the presence of vegetation (IAEA 2003).

Moisture, intense vegetation cover and lack of infrastructure in most of the Amazon region often restricts access to good rock outcrops. These features must be considered when planning an airborne-geophysical survey in such areas, and the use of airborne surveys is crucial for regional geoscientific advance. Nevertheless, in places where there are extensive deforested areas along with stripes of remaining vegetation (some of the Brazilian examples occur in the states of Rondônia, Mato Grosso, Tocantins and Pará), it is possible to verify the signal attenuation in the radioelements maps clearly marked in forest regions.

Pioneering works (Jaeger 1968; Knoll 1979) mention that to shield the gamma-ray signal, dense material or large amount of mass is required, unlike to what occurs with the

https://doi.org/10.29396/jgsb.2018.v1.n1.1
ISSN: 2595-1939

alpha and beta radiations. Thus, the densest forest may not be considered a proper “shielding material” for experimental purposes, even in fact it attenuates part of the signal. The shielding property is generally proportional to the amount of biomass, so it is expected that the denser and higher the forest, the stronger is the shielding capacity. However, recent efforts were made to estimate the efficiency of natural biomass in some microorganisms showing that there is some others non-explicit variables (Mavi et al. 2014).

Aiming at the calibration of gamma spectrometry systems in forest environments, Cresswell et al. (2018) measured gamma rays from the ^{137}Cs decay, designing a model with a canopy base less than 2 m above the ground and spacing of 2 m between wood trunks, simulating a common Japanese cedar forest. The conclusion was that in the best scenario, one sensor calibrated in open fields would underestimate the radiation measurements up to 35% into a forest with the arrangement stated above.

Therefore, the aim of this work is to estimate the magnitude of radiometric signal attenuation in rainforest regions, comparing the signal obtained for the four investigated channels of gamma-spectrometric data (Total Count - TC, potassium - K, equivalent thorium - eTh, and equivalent uranium - eU) in wooded and deforested areas and finally understand the causes of this phenomenon. For this purpose, we use a 15 x 12 km area of the Amazonian craton, in the region of Ariquemes, in the center of Rondônia State, north Brazil (Figure 1). This region is one of the most deforested areas of Brazilian Amazon (Pedlowski et al. 1997), with only near 30% of natural vegetation preserved. This phenomenon was induced by agricultural development, immigration, cattle ranching and timber extraction since mid-1970s, afterwards the launching of the Brazilian Government border occupation policy.

This area was chosen due the presence of several remaining stripes of natural vegetation juxtaposed with deforested areas with a quite simple geology, comprising Quaternary cover or weathered granite regolith. Therefore, the changing on source composition is turned into a constrained variable that allow better identification of the signal attenuation.

2. Materials and methods

2.1. Airborne gamma-spectrometry survey

The gamma-spectrometric data used in this work were derived from an airborne high-resolution radiometric and magnetic survey conducted by Lasa Prospecções S/A under the supervision of the Geological Survey of Brazil (CPRM).

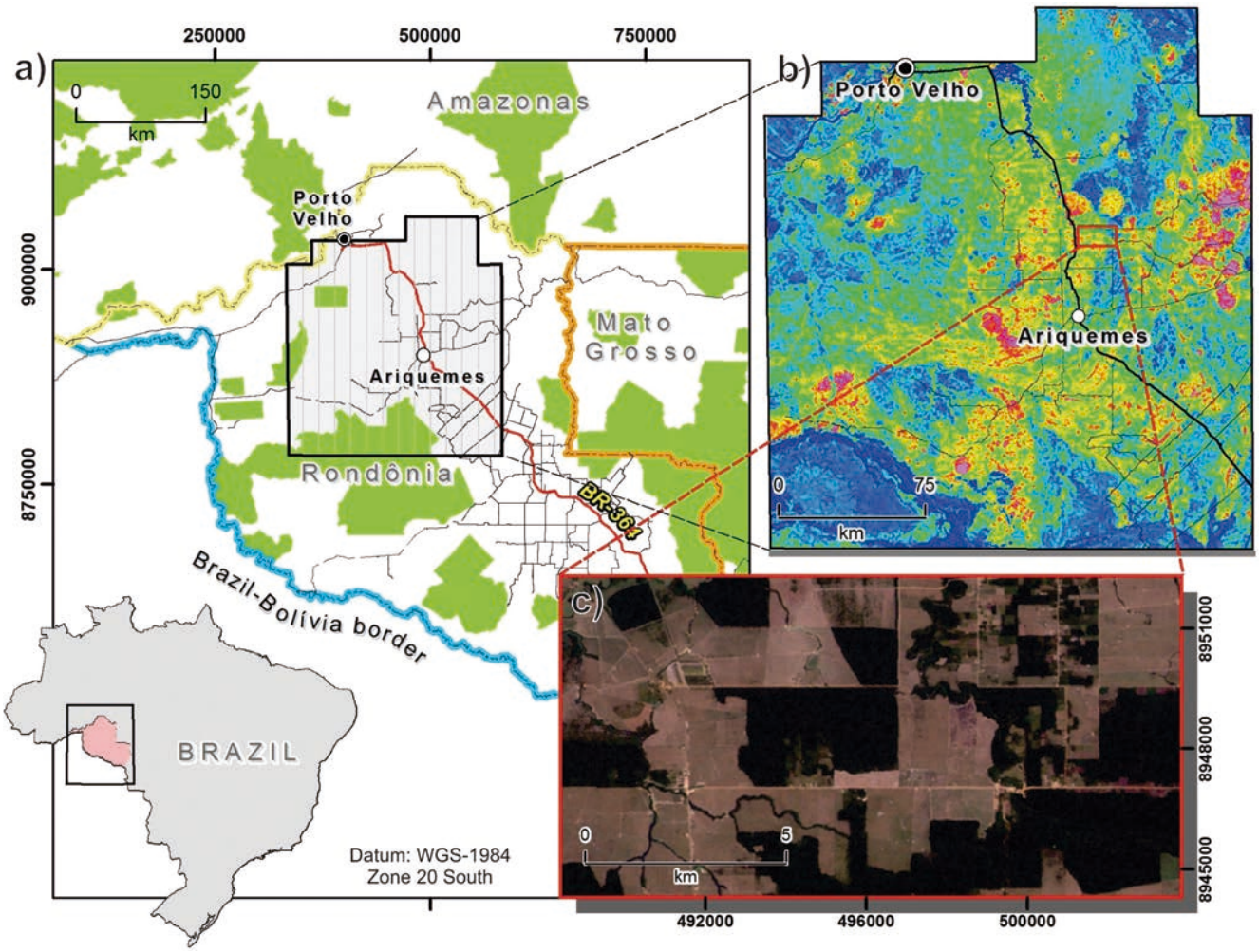

FIGURE 1 - a) Location of the airborne geophysical survey used in this work, in the central area of Rondônia State, northern Brazil. b) Total Count Radiation Map showing the localization of the study area. c) Detail of the study area in Landsat TM natural color composite showing the remaining area of natural vegetation and exposed soil, shrub and crop areas.

The survey was managed during September 2009 and April 2010 (CPRM 2010). The flight-lines were oriented in the N-S direction with 500 m between each line, and tie-lines were oriented in the W-E direction with 10 km of spacing. The nominal flight heigth was 100 m above ground surface with 15 m tolerance. An Exploranium GR-820 radiometric sensor containing 256 channels was used, and one sample was acquired for each second of surveying, which makes an average sampling distance of 75 m in line (CPRM 2010).

2.2. Normalized Difference Vegetation Index (NDVI)

The Vegetation Index (VI) is composed of robust satellite data products computed in the same way across all pixels in time and space, accessing vegetation conditions as cover, canopy and biomass, or processes such as evapotranspiration and primary productivity, and is a useful tool for indirect measures of green foliage density (Glenn et al. 2008).

One of the most common VI is the Normalized Difference Vegetation Index (NDVI), first formulated by Rouse et al. (1974), and calculated as shown in equation 1, where ρNIR and ρR are reflectance values of near infra-red and red light received at the sensor, respectively.

$$NDVI = (\rho NIR - \rho R)/(\rho NIR + \rho R) \qquad (Eq.\ 1)$$

Gizachew et al. (2016) shows the use of Landsat NDVI as a reliable tool to estimate the total biomass in forest areas and woodlands. Their work achieved a near-linear model with almost none saturation at highest NDVI values (Figure 2).

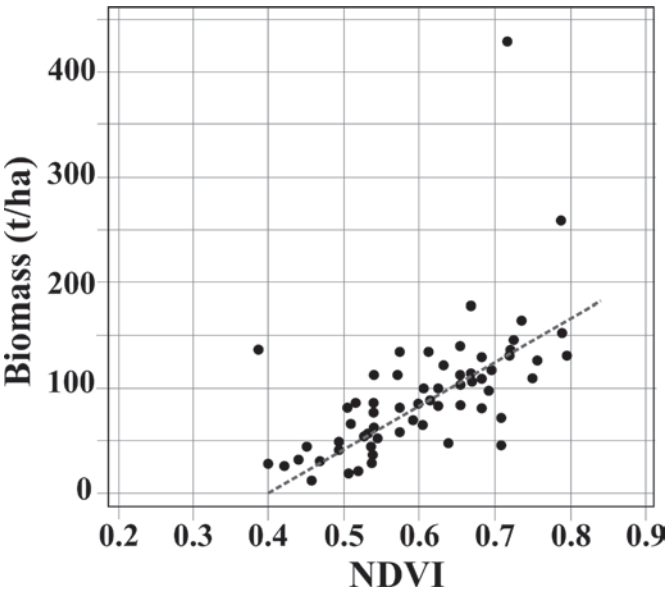

FIGURE 2 - Correlation of Total Living Biomass (TLB, in tons per hectare) and NDVI values showing a near linear model for wooded areas with none saturation (Gizachew et al. 2016).

In this work, we choose a scene of the Landsat 5 satellite Thematic Mapper sensor (TM) with 30 m of spatial resolution. The chosen scene has the address path 232, row 66 and date from May 15th, 2010, with less than 10% of cloudy cover. The scene was acquired some days after the end of the airborne geophysical survey and should not represent meaningful change in the vegetal coverage.

2.3. Digital Elevation Model

The Digital Elevation Model (DEM) used for the data processing was constructed with information collected during the airborne survey. The aircraft was equipped with a FUGRO/Enviro barometric altimeter model that provides the flight altitude with 10 meters precision. Additionally, a radar altimetry, model Collins ALT-50b, measured the flight height, compared to the land surface (canopy, buildings, and terrain) with precision of approximately 1.5 m (CPRM 2010). The difference between the altitude of flight (Alt) and the flight height (H) correspond to the DEM used for the data processing, as shown in equation 2.

$$DEM = Alt - H \qquad (Eq.\ 2)$$

For validation of these data, it was compared to NASA's 1 arc second DEM Shuttle Radar Topography Mission (SRTM), acquired in February 2000 (NASA 2013). As the SRTM, DEM also considers the canopy trees, and the main difference found in both populations correspond to those areas deforested between years 2000 (SRTM surveying date) and 2010 (airborne surveying date). These facts allow the estimation of the average height of the trees in the area as ~20 m (Figure 3).

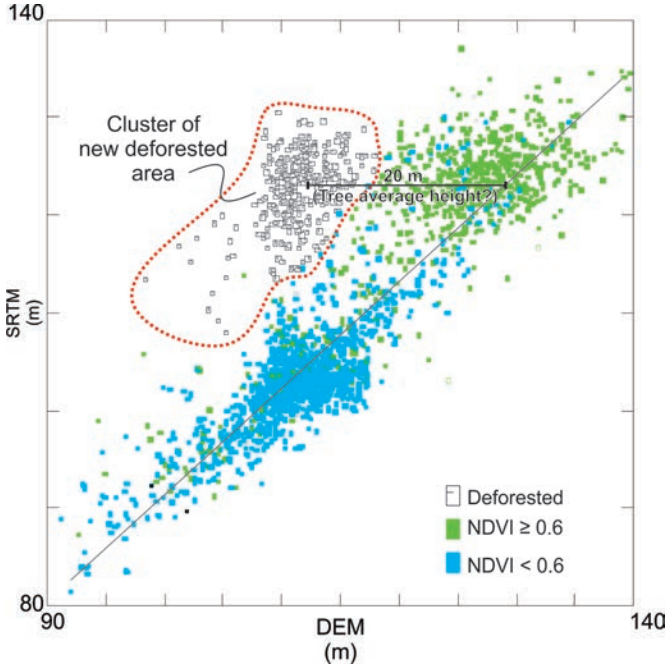

FIGURE 3 - Airborne DEM and SRTM DEM goodness-of-fit plot with moderate to strong correlation for most samples. The marked field probably corresponds to a deforested area between the two surveys. The point dispersion around the regression line is consistent with the instrumental error estimation of the elevation survey. Green rectangles represent areas with NDVI over 0.6.

3. Airborne Gamma-spectrometry processing

The airborne gamma-spectrometry data field values are influenced by many variables. Thus, it is important to correct the data in order to correlate them directly with the respective geology of the study area. First, the data must be converted into elemental count rates. This is done by correcting for dead time, energy drift and background radiation. Then, the elemental count rates are corrected for variation in the

terrain clearance of the detector and reduced to elemental concentrations in the ground (Minty 1988; Minty et al. 1997).

Besides those corrections derived from the airborne acquisition, it is also important to correct the data from the radon background contribution, stripping and height flight. The radon gas is found in the atmosphere through its escape from soils and rock fissures, thus constituting a major contributor to background radiation, especially in the U window; producing noise in the gamma-ray data. The stripping correction is used to correct each of the K, U and Th window count rates for those gamma rays not originating from their particular radioelement or decay series. For instance, thorium series gamma rays appear in both the uranium and potassium windows, and uranium series gamma rays appear in the potassium window, being relevant a specific correction for this phenomenon. Finally, the height correction is related to the nature of the airborne data acquisition, being an important attenuation factor in the gamma-spectrometry data. Due to statistical noise being greatly amplified, it is common practice to limit the height in the range 50-250 m (IAEA 1991).

The height of the detector changes continuously in airborne surveying, so the window data need to be corrected to a nominal survey height. The height attenuation is related to the energy and geometry of the source, with low-energy and narrow bodies attenuating more rapidly with distance than high-energy radiation and wide bodies (IAEA 2003). The measured count rate is related to the count at the nominal survey altitude by the equation 3:

$$N_H = N_0 . e^{-\mu H} \quad \text{(Eq. 3)}$$

where,

N_H is the count rate normalized to the nominal survey altitude H.

N_0 is the background corrected, stripped count rate at STP equivalent height H.

μ is the linear attenuation coefficient for a window.

The μ number is an important coefficient that is empirically determined, and may vary according to the capacity, size and type of the sensor crystal. Usually, this constant is defined before an airborne survey in comparison to a calibration track with ground readings (IAEA 1991). For the survey in question, the values obtained are listed in Table 1 (CPRM 2010).

Environmental particularities are also important attenuating factors, having an effect on the measured radiation. Non-radioactive overburden can significantly reduce the radiation, as well as snow cover. Soil moisture can be a relevant noise source in gamma ray survey. Uranium estimation can be greatly modified by precipitation and dense vegetation and will also have an important attenuation effect, being the trunks of trees a known responsible of a collimation effect on ground radiation. Therefore, a focused study in such a specific environment like the Amazon region is needed to generate confidential elemental concentrations of K, eTh and eU in the airborne gamma-spectrometry data.

4. Results

4.1. Data analysis

The data used in this analysis comprise four channels from gamma-spectrometric survey (Total Count, potassium, equivalent thorium and equivalent uranium), and elevation from airborne DEM and NDVI values. The data processing statistical summary is shown in Table 1. The histogram analysis of the dataset shows different patterns for each group of variables (Figure 4).

The NDVI (Fig. 4a) data shows a polymodal pattern, being possible to distinguish the rainforest peak from the non-vegetated distribution. The other two modes are concentrated in the lowest values of the Vegetation Index and in the intermediate values with a wider distribution. As the local terrain is relatively flat, the bimodal distribution in the DEM histogram (Fig. 4b) may evidence the mean difference between the height of the top of trees and the ground level. This value obtained from the difference between the two modes (18 m) is consistent with that obtained from the comparison of the airborne DEM and SRTM in deforested areas shown in section 2.3.

The equivalent thorium populations show an asymmetric, right skewed, unimodal distribution (Fig. 4c), and with the median value being 3 times lower than that that of the highest value. Since thorium is considered the less mobile radioelement, and the local area is significantly weathered, this variation may reflect some remaining composition from the rock source. For the wooded area, the trend is similar, but with lower values. The Total Count (Fig. 4d) signal follows the same pattern due to the high correlation with the equivalent thorium responses.

K and eU have shown a quite symmetric unimodal distribution (Fig. 4). For K (Fig. 4e), the range of values is very small, and the negative values are probably due to bad noise-to-signal ratio. The mean value and the mode are near 0.1%, with the maximum almost reaching 0.6%. When comparing the histograms for wooded and non-vegetated areas, there is a slight but not clear attenuation of the mode and maximum values. For the eU histogram, it is possible to identify a concise reduction in the maximum and minimum values (Fig. 4f). The eU concentration range varies from 0 to 6 ppm.

In order to support the comparison, the NDVI population was divided into four equal intervals spaced in values of 0.2 (Table 1). The first interval (0.01-0.20) sets to regions of soil or rock exposure, the second interval (0.21-0.40) corresponds to shrub, grass or pasture areas, the third interval (0.41-0.60) stands for farming, crop or harvest while the fourth interval (0.61-0.80) shows a good fit to the rainforest area. This last interval is responsible for approximately 45% of the study area, while the non-wooded area corresponds to the remaining interval (0.00-0.60).

4.2. Map interpretation

The maps were drawn by the interpolation of values according to the sample spacing specificity of each survey. All maps were interpolated using the Minimum Curvature method (Briggs 1974) and are displayed in UTM coordinates, datum WGS 1984, zone 20 south. The Landsat NDVI and the SRTM DEM maps were interpolated with 30 meters intervals with no blanking distance. The TC, K, eTh and eU maps were interpolated using 125 meters intervals (Figure 5).

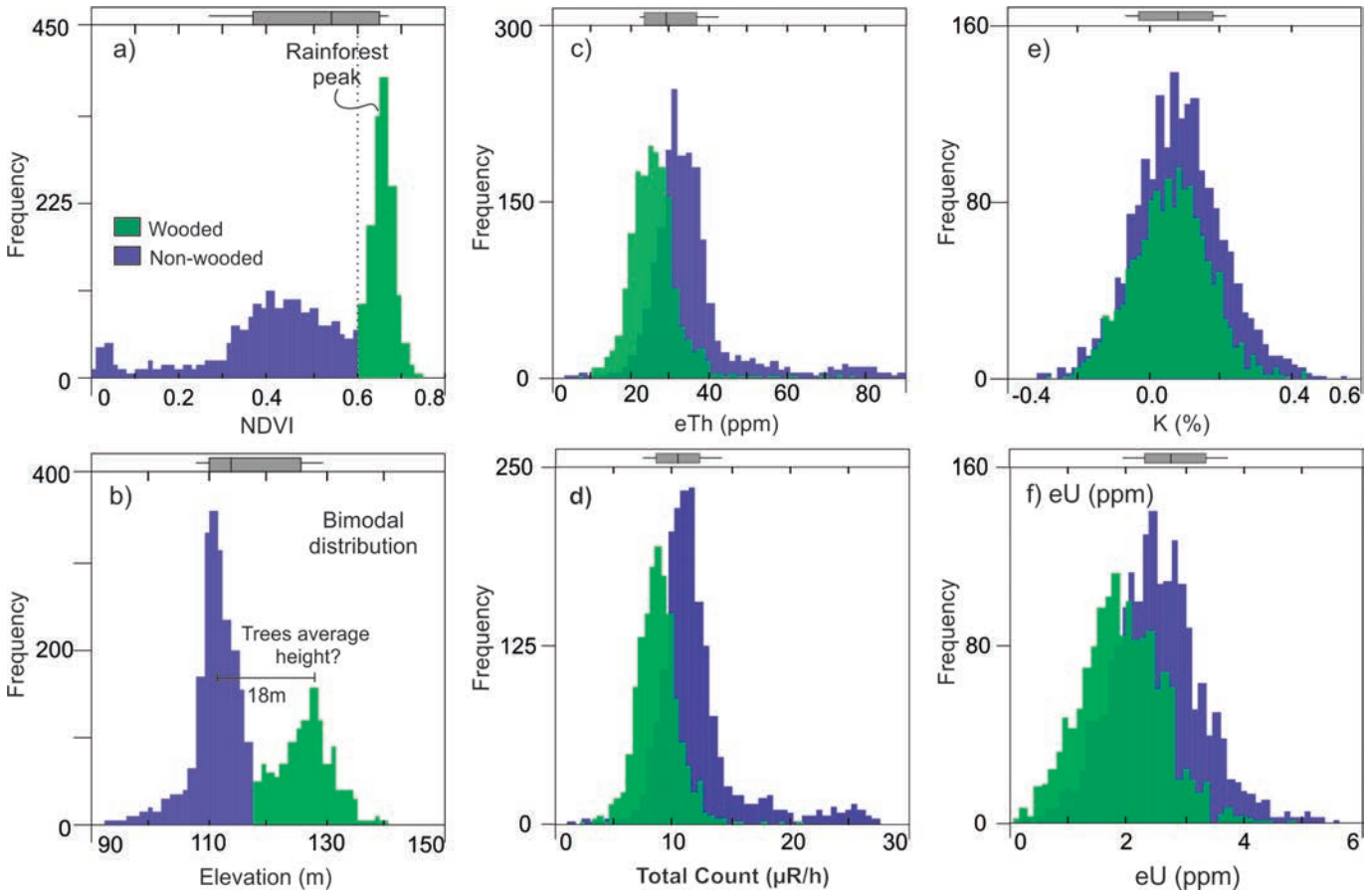

FIGURE 4 - Set of histograms and data box-plot. a) NDVI histogram showing a 0.7 peak attributed to rainforest, b) Elevation histogram with bimodal distribution. The major peak is around 110 m and the secondary peak is around 130 m. This is attributed to the difference between the average ground level and the average canopy height, c) and d) asymmetric distribution for wooded (green) and non-vegetated (purple) areas for eTh and TC, respectively; e) and f) unimodal symmetric distribution with small range of values for K and eU, respectively

TABLE 1 - Statistic summary of the gamma-spectrometric and elevation data classified by NDVI group and respective linear attenuation coefficient (µ) from the survey.

		NDVI: 0.00-0.20			NDVI: 0.21-0.40			NDVI: 0.41-0.60			NDVI: 0.61-0.80		
		Soil or rock (n=240)			Pasture or shrub (n=580)			Crop or harvest (n=1036)			Rainforest (n=1476)		
	µ (1/m)	Mean	Max	Min	Mean	Max	Min	Mean	Max	Min	Mean	Max	Min
Total Count	-0.0071	13.67	27.09	6.79	12.78	27.63	2.98	11.43	25.94	1.33	8.77	24.21	2.41
K (%)	-0.0089	0.09	0.47	-0.30	0.08	0.55	-0.32	0.09	0.50	-0.28	0.08	0.46	-0.25
eTh (ppm)	-0.0068	40.96	85.82	18.97	38.26	89.48	8.09	33.77	83.18	3.85	25.72	76.56	6.65
eU (ppm)	-0.0080	2.72	4.15	0.64	2.57	5.57	0.49	2.46	5.16	0.27	1.93	4.84	-0.48
DEM (m)	-	111.7	128.6	95.8	111.7	131.1	93.2	112.1	134.5	91.2	122.4	144.0	92.7

The correlation between the NDVI and high elevation values with the low radioelements concentration is evident in the maps of the figure 5. The NDVI map (Fig. 5a) shows the polygonal patterns of rainforest areas and aired soil, road and pasture. Based on this, the hatched areas were delimited to support the interpretation of the radioelements maps.

The SRTM DEM map (Fig. 5b) shows that the area's relief is relatively flat, with some shallow valleys draining towards the north. The main elevation of the terrain is around 110 meters. In addition, except for the small valleys, the only topographic variations are concentrated on small hills in the southwest and northwest sectors of the area. The forest areas have elevations up to 150 meters.

The TC (Fig. 5c) and eTh (Fig. 5e) maps show strong attenuation in forested areas and are associated with NDVI high values (Fig. 5a). In contrast, TC and eTh high concentrations are related to the NDVI lowest values. Towards the west, there is a substantial increase of the response correlated to the hills areas, which probably means a change on the radiation source. Those areas are identified as regolith cover over highly weathered granite domains. This is endorsed by the values of eU and K, not different from the background.

The eU and K maps are noisier than the others are, as shown in the histograms (Fig. 4e and 4f). In the K (%) map (Fig. 5d), there is a poor distinction between background values and outliers. This occurs because the total amount of K in the source is so low, probably due to K depletion, such that the signal is almost below the detection limit, which increases the proportion of noise in the final product. Even then, it is possible to notice some attenuation in the western part of the area, where the radiation values are somewhat higher than the background. In the eU map (Fig. 5f), the relationship between background, noise and signal is clearer, and it is possible to visually estimate the attenuation on the marked areas.

Therefore, the Total Count (Fig. 5c) map is a suitable representative of the local radiation and it can be used for comparison purposes in diagrams that consider the elevation and forest relationship (Figure 6).

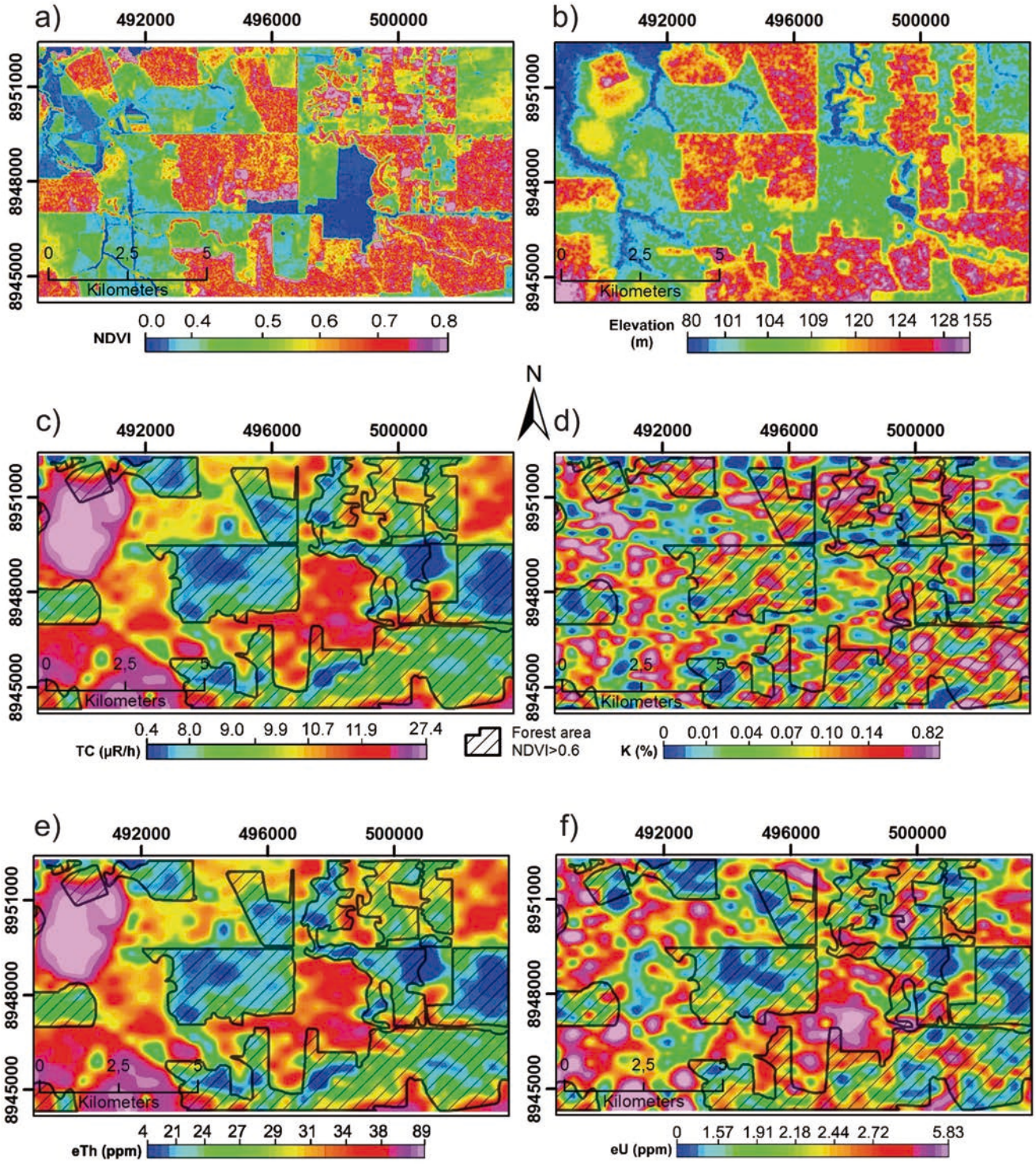

FIGURE 5 - Maps based on interpolation of values calculated by the Minimum Curvature method. The hatched areas of wooded contour were drawn by delimiting NDVI values greater than 0.6. The respective color bar is below each map; a) 30-meter pixel NDVI map; b) 30-meter pixel SRTM DEM; c) Total Count map with 125-m pixel, as well as the next; d) K (%) map; e) eTh map; f) eU map.

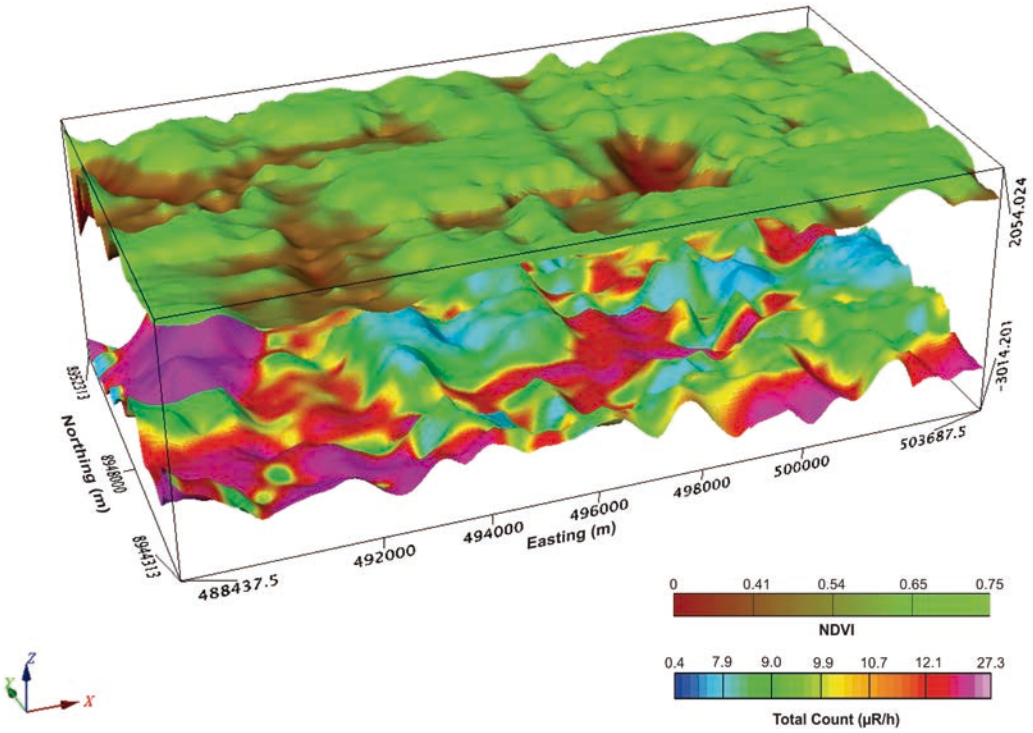

FIGURE 6 - Three-dimensional comparison of NDVI and TC maps. The vertical scale of the TC map is based on airborne DEM values

5. Discussion

5.1. Underestimation of source distance

The total amount of radiation presents an exponential behavior as a function of the distance, as shown by Equation 3. As the radar used in the survey could not pass through the treetops, the real distance between the source of radiation and the sensor is underestimated during the processing (Figure 7).

Thus, if we replace the µ values in Eq. (3) by those stated in Table 1 and estimate the tree height as shown in the observations of sections 2.3 and 4.1, we may find an average underestimation of 13% of the signal in the data processing, which can increase towards the final concentration result by error propagation. This unwanted effect can be avoided by the improving of the Digital Elevation Data, which should consider only the real terrain for this calculation. As in most regions, it is hard to estimate the mean tree height, the transformation from a digital elevation model into a digital terrain model remains an arduous task. However, without this correction, the dataset is impaired to more accurate quantitative analysis.

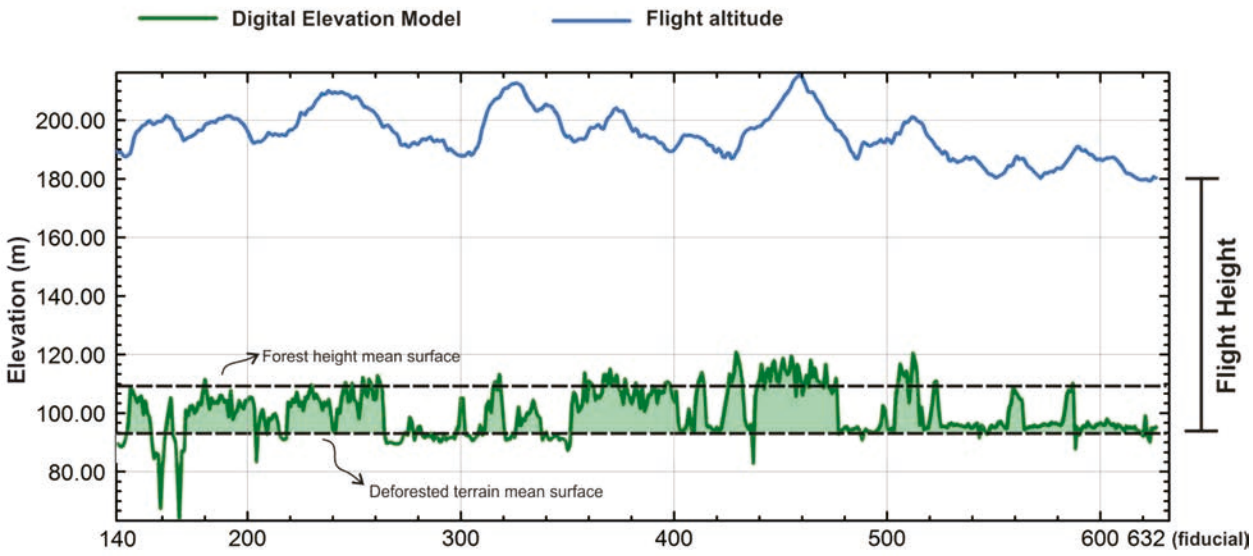

FIGURE 7 - Flight height compared to digital elevation model. The real distance between the source and the sensor is underestimated because the radar used in the common surveys considers the canopy tree as the ground surface.

5.2. Underestimation in radioelement concentration

As shown in this work, radioelements responses tend to decrease as the amount of biomass in forest regions increases, which consequently increases the NDVI values. Therefore, the NDVI value can be used to estimate the attenuation coefficient (Figure 8).

Simplifying, the total linear attenuation can be calculated as a normalization of the mean values of radiation in non-vegetated areas and the mean values of radiation in wooded areas. Accordingly, using the values shown in Table 1, we reach the estimation of total attenuation in radioelement concentrations of 37% for eTh, 29% for eU and 12% for K (%). For the Total Count channel, the attenuation estimative is 36%.

6. Final remarks

As the ideal geophysical product must rely only on the variation in geological parameters from the studied object (rock, soil or other natural material), the vegetation constitutes a major problem since it greatly affects the radiometric signal and may cause geologic misinterpretation in studies based on the data. The use of radiometric data in mineral exploration, environmental or geological mapping can be a good alternative for a fast and relatively cheap solution in a research. Nevertheless, for a good interpretation, the interpreter should consider consulting other information, such as the terrain variation and the vegetal cover.

The attenuation discussed in this paper has a natural cause and is very common in areas of high amount of biomass in dense forest. Outside the Amazon region, minor attenuation can be verified in several areas of reforestation for commercial purposes existing in the whole country. For other natural common causes of radiometric signal attenuation, such as snow, the researchers have reached to some routines that minimized the question, but the vegetal cover attenuation remains open.

The application of direct correlation by linear regression does not seem to be the best way to solve this issue, because even in an area with controlled geology, as shown in Figure 8, the correlation exists and can be measured, but the dispersion of the values is large, adding more uncertainty to the final product. The solution may involve the use of robust decorrelation matrices between the NDVI values and the radiometric maps.

The Landsat NDVI parameter seems to be a good control population for the integration between the radiometric maps and the vegetation cover. However, as the total amount of green leaves varies throughout the seasons, even in the Amazon region, the researcher should weigh between the

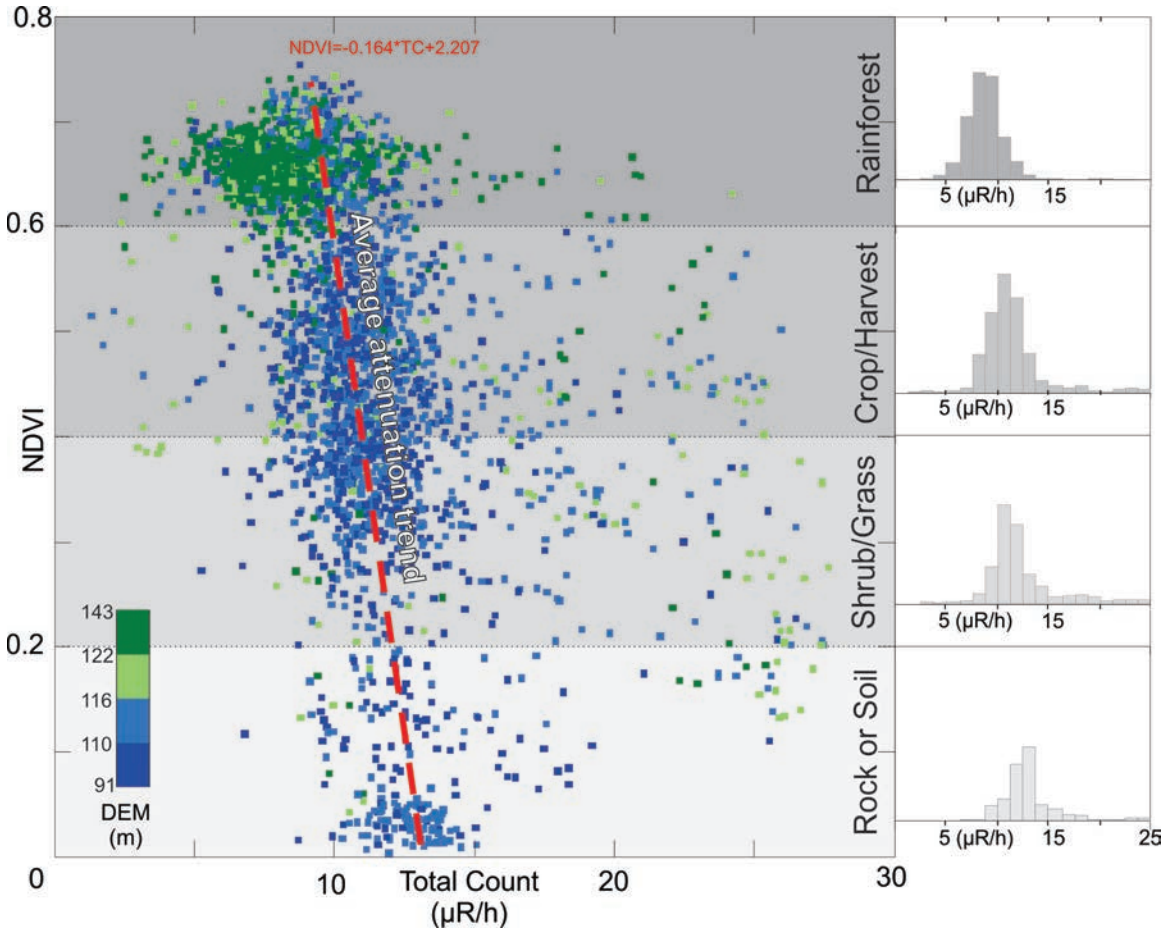

FIGURE 8 - Total Count (μR/h) scatter plot from NDVI. The dots are colored according to the elevation obtained in the airborne DEM (see the legend). The NDVI intervals are divided by the correspondent vegetation classes. It is possible to notice an attenuation average trend from the rainforest to the soil samples. Most of the DEM highest values are concentrated above the NDVI 0.6 line. To the right, the histograms of each interval for TC values are shown.

rainy season, with the highest percentage of green leaves, and the cloud cover. In Rondônia State, the month of May seems to show the best set, unlike the months between July and October.

In a general way, up to one third of the radioelement concentration is underestimated in the rainforest areas because of the signal retention. In completely wooded areas, it may not be a problem for delimitation of radiometric domains or for other qualitative analysis, since there will be no lateral changing on attenuation. However in deforested regions, where some forest areas remain, some attenuation and false variations in may appear in the maps, and an unwary interpreter can trace geological limits that do not exist, or in the opposite way, some reserve forest area could disguise a radiometric anomaly of a mineral deposit.

Acknowledgements

The authors would like to thank Roberto Gusmão de Oliveira and Luiz Gustavo Pinto for the preliminary considerations about the data analysis and the content of the original idea. David Lopes de Castro and Francisco José Fonseca Ferreira were the kind reviewers who made valuable suggestions on the paper. GFS would like to thank to Anderson Dourado and Dalton Valentim for reading and writing suggestions about the original manuscript.

Supplementary dataset

The set of raw data used in this work are available on the web at the following address: https://www.researchgate.net/publication/323343017_Raw-data_Gamma-ray_attenuation_caused_by_rainforest_dispersion_compared_to_Vegetation_Index_estimates_on_the_effects_of_airborne_gamma-spectrometry_data

References

Beamish D. 2015. Relationships between gamma-ray attenuation and soils in SW England. Geoderma, 259, 174-186.

Bedini E., Rasmussen T.M. 2018. Use of airborne hyperspectral and gamma-ray spectroscopy data for mineral exploration at the Sarfartoq carbonatite complex, southern West Greenland. Geosciences Journal, 23, 1-11.

Briggs I.C. 1974. Machine contouring using minimum curvature. Geophysics, 39, 39-48.

Cresswell A.J., Sanderson D.C.W., Yamaguchi K. 2018. Assessment of the calibration of gamma spectrometry systems in forest environments. Journal of Environmental Radioactivity, 181, 70-77.

Elkhadragy A.A., Ismail A.A., Eltarras M.M., Azzazy A.A. 2016. Utilization of airborne gamma ray spectrometric data for radioactive mineral exploration of G.Abu Had – G.Umm Qaraf area, South Eastern Desert, Egypt. NRIAG Journal of Astronomy and Geophysics, 6, 148-161.

Gizachew B., Solberg S., Næsset E., Gobakken T., Bollandsås O.M., Breidenbach J., Zahabu E., Mauya E.W. 2016. Mapping and estimating the total living biomass and carbon in low-biomass woodlands using Landsat 8 CDR data. Carbon Balance and Management, 11, 1-13.

Glenn E., Huete A., Nagler P., Nelson S. 2008. Relationship Between Remotely-sensed Vegetation Indices, Canopy Attributes and Plant Physiological Processes: What Vegetation Indices Can and Cannot Tell Us About the Landscape. Sensors, 8, 2136-2160.

IAEA 1991. Airborne gamma ray spectrometer surveying. Vienna, International Atomic Energy Agency, 130p.

IAEA 2003. Guidelines for radioelement mapping using gamma ray spectrometry data. Vienna, International Atomic Energy Agency, 179p.

Iza E.R.H.F., Horbe A.M.C., Silva A.M. 2016. Boolean and fuzzy methods for identifying lateritic regoliths in the Brazilian Amazon using gamma-ray spectrometric and topographic data. Geoderma, 269, 27-38.

Jaeger RG. 1968. Engineering compendium on radiation shielding: volume I, Shielding fundamentals and methods. Berlin, Springer Verlag, 423 p.

Knoll G.F. 1979. Radiation Detection and Measurement. New York, John Wiley and Sons Inc., 816 p.

CPRM - Serviço Geológico do Brasil. 2010. Projeto Aerogeofísico Rondônia Central: relatório final do levantamento e processamento dos dados magnetométricos e gamaespectrométricos. Programa Geologia do Brasil (PGB), Rio de Janeiro: Lasa Prospecções, 26v., v.1.

Mavi B., Gurbuz F., Ciftci H., Akkurt I. 2014. Shielding Property of Natural Biomass Against Gamma Rays. International Journal of Phytoremediation, 16, 247-256.

Minty B.R.S. 1988. A review of airborne gamma-ray spectrometric data-processing techniques. Bureau of Mineral Resources, Geology and Geophysics, Report No. 255.

Minty B.R.S., Luyendyk A.P.J., Brodie R.C. 1997. Calibration and data processing for airborne gamma-ray spectrometry. AGSO Journal of Australian Geology and Geophysics, 17, 51-62.

NASA 2013. NASA Shuttle Radar Topography Mission United States 1 arc second. Version 3. 10°S, 63°W. Available: < https://lpdaac.usgs.gov/node/523>.

Pedlowski M.A., Dale V.H., Matricardi E.A.T., Silva Filho E.P. 1997. Patterns and impacts of deforestation in Rondônia, Brazil. Landscape and Urban Planning, 38, 149-157.

Perrotta M.M., Almeida T.I.R., Andrade J.B.F., Souza Filho C.R., Rizzotto G.J., Santos M.G.M. 2008. Remote sensing geobotany and airborne gamma-ray data applied to geological mapping . In: The International Archives of the Photogrammetry, Remote Sensing and Spacial Information Sciences, 1, 1275-1280.

Rouse J.W.J., Haas R.H., Schell J.A., Deering D.W. 1974. Monitoring Vegetation Systems in the Great Plains with Erts. In: Third Earth Resources Technology Satellite Symposium, 1, 309-351.

Saad M.H. 2017. Measurement and Analysis of Airborne Gamma–Ray data For Geological Mapping and Mineral Exploration. IOSR Journal of Applied Physics, 9, 69-77.

Shives R.B.K. 2015. Using gamma ray spectrometry to find rare metals. In: Simandl G.J., Neetz M. (eds.) Symposium on Strategic and Critical Materials Proceedings, British Columbia Geological Survey Paper, 2015-3, 199-209.